Fiber-Reinforced Concrete Walls Using Insulated Formwork

Design method applies advanced technology to residential construction

BY RONALD F. ZOLLO AND CAROL D. HAYS

Fiber-reinforced concrete (FRC) has gained widespread acceptance as a suitable construction material for a wide variety of nonstructural applications. There has been little achieved in the development of analysis and design procedures, however, that capitalize on the engineering properties of FRC. This article includes a design example of residential FRC walls built using stay-in-place insulating concrete forms (ICF). This combination of materials is given the acronym ICF-FRC.

Important FRC material properties that relate to its performance include post-cracking tensile strength and toughness. It is FRC's tensile behavior under static, impact, and cyclic loading that makes it superior in many applications. Compression behavior of FRC does not significantly differ in comparison with plain, ordinary portland cement concrete. A reliable measure and a practical design parameter for FRC tensile behavior is the average residual strength (ARS), determined by ASTM C 1399 "Test Method for Obtaining Average Residual-Strength of Fiber-Reinforced Concrete." The following demonstrates how ARS and conventional engineering design methods, such as working stress or ultimate strength, can be used to produce building code-compliant ICF-FRC wall systems.

ICF SYSTEMS

ICF systems use polystyrene or similar foam cellular materials as vertical formwork for field-cast concrete walls. The walls in the current example are solid planar walls. When used in residential construction, the insulating formwork panels are finished on the building's interior and exterior surfaces using conventional techniques. As a structural system, ICF walls currently use either structural plain concrete (ICF-P), designed according to Chapter 22 of the ACI 318-02 "Building Code Requirements for Structural Concrete," or structural reinforced concrete (ICF-R), designed according to ACI 318-02 Chapters 9 through 12.

There are practical limitations associated with the ICF-P and ICF-R systems. Limitations associated with ICF-P include: the unreliability of the modulus of rupture (MOR) of plain concrete as a design parameter and, as an essentially brittle material, plain concrete's lack of contribution to the wall's structural integrity with regard to static overload, dynamic impact, or cyclic loading conditions. In the case of ICF-R, there are limitations associated with placing horizontal and vertical reinforcement and, thereafter, placing the concrete within the formwork cavity. Nevertheless, both ICF-P and ICF-R designs, which meet ACI requirements, have been successfully applied in housing construction.

By comparison, FRC appears to avoid the limitations ascribed to both ICF-P and ICF-R systems. This is due to FRC's reliable post-cracking strength and ductility, and on its ability to largely, if not entirely, eliminate the need for continuous reinforcement armatures in wall systems.

The following design example shows how ICF-FRC walls can satisfy both conventional reinforced concrete (RC) and plain concrete design standards represented by ACI 318 (Chapters 9, 10, 11, 12, and 22) and the Florida Building Code (FBC).

DESIGN METHOD RATIONALE

We propose applying the principles of plastic analysis and design to ICF-FRC. Yield line theory, as applied to RC, is one such example. Plastic analysis has long been recognized as a rational method for structural design. This approach recognizes the fact that structures can be designed to perform suitably when local plasticity and force redistribution are permitted. Such designs generally result in improved design efficiency without sacrificing safety or structural integrity. Force redistribution and contained plastic flow (cracking) are exactly what occur when load is applied in both conventional RC and in FRC, even if the mechanisms are different. In RC, structural integrity fundamentally depends on a load path that is contained within the ductile structural armature (the reinforcing steel). In the FRC, structural integrity is dependant on a load path that is maintained in the pseudo-ductile binder and fiber materials. It seems appropriate to differentiate between conventional RC and FRC as the former being a structural system and the latter being a material system. We believe this distinction is often not considered or not understood well enough by design engineers.

Underlying the plastic design approach to structural safety are the so-called static and kinematic theorems, formally expressed by B. G. Neal.[1] In the context of the current discussion, these theorems require simply that any set of factored loads applied to a structure (any load case) satisfy two conditions: the external loads produce a distribution of internal forces that satisfies equilibrium; and any localized regions of contained plastic flow (yielding or cracking) are not sufficient to form a collapse mechanism for any part of the structure. When these two conditions are satisfied for all parts of the structure, then the loading is, and must be, less than the collapse (failure) load for the structure. In brief, by the static theorem, a structure can demonstrate its safety (not in danger of collapse) and, thereafter, need only to satisfy serviceability requirements such as limitations on deflections, wind-borne projectile resistance, and the effect of load cycles or reversals to ensure an acceptable structural design.

The current example demonstrates the ICF-FRC wall design procedure using two analytical approaches that are common to engineering practice: semi-empirical strength of materials (SOM) analysis and elastic, or modified elastic-plastic, finite element method (FEM) analysis. In FEM, a house is modeled either as a fully elastic structure, with no substantial yielding (cracking) predicted, or as a model that incorporates local yield line growth, when yield lines are predicted to occur. In any case, materials are assumed to behave in an elastic-perfectly-plastic mode of flexural behavior. This is a valid description of the behavior of either RC structural elements or FRC materials after localized cracking and reloading has occurred (when limited to small deformations).

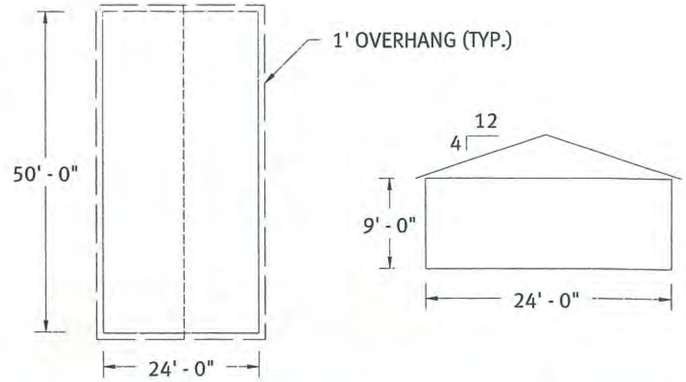

Fig. 1: Plan and elevation views of ICF house used in the design example (1 ft = 0.305 m)

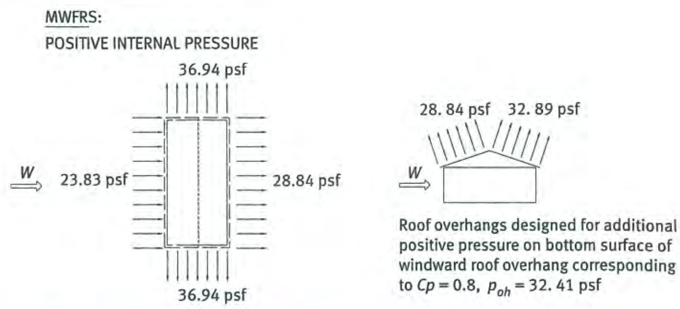

Fig. 2: Wind loads calculated for the main wind force resisting system of the design house, considering positive internal pressure only (1 psf = 47.9 Pa)

ICF-FRC DESIGN EXAMPLE

The current FBC, Miami-Dade County regional edition, is applied in this design example. This code is a particularly high-level design standard in regard to lateral, uplift, and impact loading caused by wind and wind-borne debris. The FBC incorporates ASCE 7-98 "Minimum Design Loads for Buildings and Other Structures." The example demonstrates how ICF-FRC satisfies the requirements of structural integrity between elements of the building envelope, roof, walls, and foundation. Resistance to penetration damage from wind-borne debris is expected for ICF-FRC system design, but is not investigated as part of this article.

Exemplar house description

A simple rectangular house plan enclosing a 24 by 50 ft (7.3 by 15 m) area is used in this example. It has a ridge roof line parallel to the 50 ft (15 m) dimension with a 9 ft (3 m) eave height. The roof is a hip construction with a pitch of 4:12. Roof diaphragm action is assumed as a means of lateral support at the top of the perimeter walls. For this example, concrete compressive strength f_c' is assumed to be 3 ksi (20 MPa). Figure 1 shows the house plan elevation views. It is assumed that the house is located in exposure category C, as defined by ASCE 7-98, with the following design parameters applied for determination of wind loads. Wind speed V is 148 mph (65 m/s); structure category is II; it is an enclosed building, so the internal pressure coefficient GC_{pi} is ±0.18; and velocity pressure q is 47.66 lb/ft^2 (2.3 kPa). Figure 2 shows the resulting wind loads calculated for the main wind force resisting system (MWFRS), considering only positive internal pressure (to simplify and shorten the discussion). The requirements of the FBC and ASCE 7-98 regarding the forces on building components and cladding are applied later in the analysis.

Structural models

A 3-D model was used for the MWFRS and a 2-D model for forces on components and cladding. Comparing these two models (for the same design parameters) proved that the 2-D analysis could be used to predict the distribution of internal forces at critical points of the wall structure. Nevertheless, the 3-D model for the MWFRS is used in this discussion as it best demonstrates graphically the results of the FEM analysis. The 3-D plate element nodes are spaced at 2 ft (600 mm) on center horizontally and 1.8 ft (550 mm) on center vertically. The house has openings covered by doors and windows that transfer forces caused by wind pressure to the walls but don't contribute any strength to the walls.

Figure 3 shows the model with the support conditions symbolized. Support conditions at the bottom of the walls are assumed to be fixed. This condition is intended to model the construction connection between the walls and the footing, which consists of No. 5 reinforcing bars continuing vertically from the foundation and into the ICF-FRC walls. Truss connections at the top of the walls are at 2 ft (600 mm) on center and provide lateral reactions perpendicular to the walls and uplift resistance.

FEM wind-load analysis of the MWFRS

Assuming 4-in.-thick (100 mm) ICF-FRC walls, FEM analysis provides a qualitative deflection diagram (Fig. 4) for the MWFRS. Figure 5 and 6 show the horizontal and vertical moment force distributions. Wind-load analyses were run for the cases of wind on flexible side walls and wind on rigid side walls (to obtain worst case moment distributions for windward and leeward walls). For brevity, only the results for the flexible side walls are presented. Figure 5 demonstrates the M_x moments when the wind force is applied to the entire structure, which (using the right hand rule) are those plate edge moments that are parallel to a horizontal axis in the plane of the wall. Figure 6 shows the M_y moments, which are plate edge moments that are parallel to a vertical axis in the plane of the wall. Figure 7 shows the maximum principal stresses on the face of the plate elements for the loading case of wind applied to the entire structure.

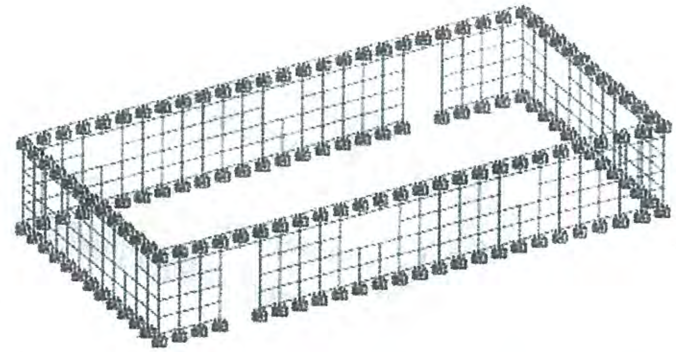

Fig. 3: Wall supports for the model of the full structure main wind force resisting system

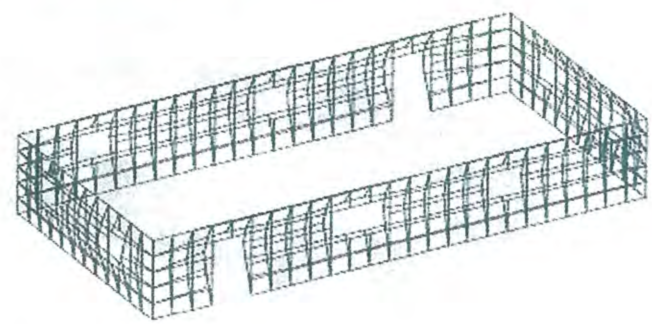

Fig. 4: FEM model of the deformed structure after loading with 148 mph (65 m/s) wind

Color patterns on Fig. 5 through 7 represent levels of either moment force or principal stress for the MWFRS loading condition (assuming flexible side walls and positive internal pressure). These results, and comparisons with other load conditions and models such as rigid side walls, lead to the following conclusions for the windward wall forces and stresses.

1. Plate element moments M_x and reaction forces along the bottom of the wall (the latter are not shown in this article) show that the maximum M_x moment and moment reaction forces occur when the side shear

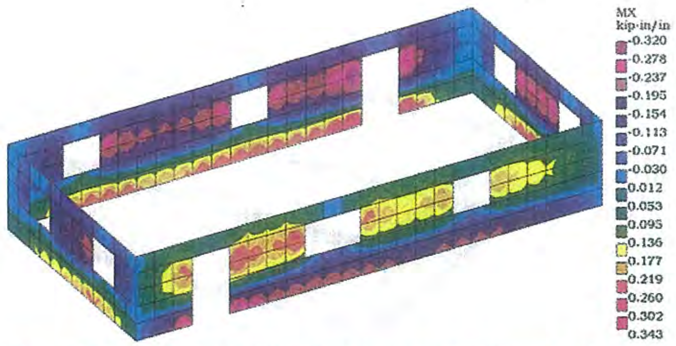

Fig. 5: Moment force distribution about the horizontal axis calculated from the FEM analysis (1 k-in./in. = 4.45 kN-m/m)

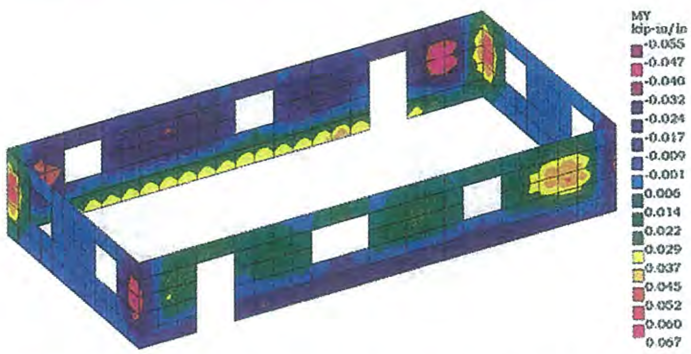

Fig. 6: Moment force distribution about the vertical axis calculated from the FEM analysis (1 k-in./in. = 4.45 kN-m/m)

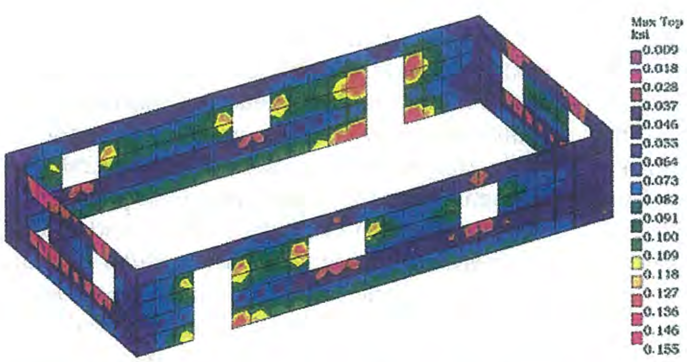

Fig. 7: Maximum principal stresses (caused by bending) on the face of the plate elements for the loading case of wind applied to the entire structure (1 ksi = 6.89 MPa)

walls are free to deform, as in the flexible side wall model.

2. Maximum plate element moments M_y along the side edges of the windward wall occur when the side walls are assumed rigid, that is, when the side wall edges are fixed against rotation about the vertical axis. The maximum M_y plate moments at the corners of the leeward wall, however, occur when the side walls are flexible and the corners are free to rotate.
3. Maximum moments in highly stressed areas of the wall are not necessarily oriented parallel to either the x or y axis, such as near re-entrant corners at openings where yielding (cracking) might be expected to occur. These maximum moments can be estimated based on a free body analysis of the plate elements and the M_x and M_y moments for the particular plates and loading case. The principal stress distribution can also be used to determine locations of maximum bending stress.
4. Reaction moment forces along the bottom of the windward wall found for a node spacing of 2 ft correlate well with the moment forces parallel to the bottom of the wall elements that are given on a per foot basis. These reaction forces, as well as uplift reaction forces, are used to design the vertical reinforcing bar at the connection of the wall to the footing. For an assumed No. 5 reinforcing bar at 2 ft (600 mm) spacing, the fully plastic (or theoretical ultimate) moment (based on an effective depth of 2 in. [50 mm] with f'_c = 3 ksi [20 MPa]) is 1.3 k-ft/ft (5.8 kN-m/m). This exceeds the highest value of M_x reaction force predicted by the FEM elastic model at any point along the bottom of any wall used in this example. Thus, at least for the MWFRS, yielding (or yield line development) would not be expected along the line adjacent to the foundation.
5. The maximum M_y moment at a corner of the house was found to be 0.13 k-ft/ft (0.6 kN-m/m). This value is less than what is required to crack a 3 ksi (20 MPa), 4-in.-thick (100 mm) wall using either a MOR value of $7.5\sqrt{f'_c}$ = 0.41 ksi (2.8 MPa) or, according to ACI Eq. (22-2), $5\sqrt{f'_c}$ = 0.27 ksi (1.9 MPa). Thus cracking (yield lines) along vertical wall corners will not be expected. Even if cracking does occur at wall corners, however, the fully plastic moment capacity of the FRC, based on ARS of 0.20 ksi (1.4 MPa) and a wall thickness h of 4 in. (100 mm), provides a moment capacity of

$$M = 2.0h^2 \text{ (ARS)} = 0.53 \text{ k-ft/ft (3.7 kN-m/m)}$$

which still exceeds the moment found in the example analysis.

Design alternatives

So far in this example, no yield lines are predicted. One of the following four design alternatives is available when yield lines are predicted.

First, the analytical model can be altered to one that includes yield lines. The revised model would have rotational releases along predicted yield lines and an applied joint load (constant moment) opposite to the yield line rotation. The magnitude of these applied moments is determined based on a presumed or design value of the fully plastic moment associated with the FRC (based on ARS). Full wind loading would be applied in the revised analysis and if no collapse mechanism is caused to occur then, according to the static theorem of plastic analysis and design, the applied loading is guaranteed to be less than the collapse load for the structure. The serviceability requirements can then be checked.

Another alternate approach is to increase the wall thickness, which decreases the bending stresses that predict cracking when compared with the MOR of the concrete. For example, for the 3-D elastic model in the present example, an analysis run with a 6 in. (150 mm) wall thickness indicates that the moment required to reach the ultimate strength at the base of the windward wall using a single No. 5 reinforcing bar at 2 ft (600 mm) on center is 1.99 k-ft/ft (8.9 kN-m/m), compared with 1.29 k-ft/ft (5.7 kN-m/m) for the 4 in. (100 mm) wall. The fully plastic moment for FRC with ARS of 0.20 ksi (1.4 MPa) in a 6 in. (150 mm) wall is 1.2 k-ft/ft (5.3 kN-m/m), compared with 0.53 k-ft/ft (2.4 kN-m/m) for the 4 in. (100 mm) wall.

Third, and unrelated to the use of FRC, the somewhat unreliable MOR (cracking stress) of the concrete can be increased by increasing f'_c to avoid yield line formation.

Finally, the fully plastic moment resistance of the FRC can be increased for any given wall thickness by specifying a higher ARS requirement. This is done by determining ARS for mixture proportions using a higher fiber concentration or a different fiber type.

EXAMPLE ICF-FRC DESIGN PROCEDURE

Minimum wall thickness ICF-P walls

ACI 22.6.6.2 requires the minimum wall thickness $h_{min} = \ell_u/24$ or 5.5 in. (140 mm). In this example, the unsupported wall length ℓ_u = 108 in. (2.7 m).

$$\therefore \ell_u/24 = 108/24 = 4.5 \text{ in. } (110 \text{ mm}) < 5.5 \text{ in. } (140 \text{ mm})$$

Minimum wall thickness ICF-R walls

No minimum thickness is prescribed for walls designed rationally as compression members (ACI 14.4), but empirical design (ACI 14.5) requires a minimum 4.0 in. (100 mm) or $\ell_u/25$. Also, where appropriate, slenderness effects must be considered. A check for slenderness (ACI 10.12.2) for walls in a non-sway frame (k = 1.0) is demonstrated as follows; where M_1 is the smaller factored end moment on a compression member; M_2 is the larger factored end moment on a compression member; and r is the radius of gyration of the compression member's cross section.

From ACI Eq. (10-7):

$$k\ell_u/r \le 34 - 12(M_1/M_2), \text{ with } M_1 = 0 \text{ and } r \approx 0.3\ell_u,$$
$$k\ell_u/r = 90 > 34$$

∴ Slenderness must be considered in further analysis.

Wall shear capacity

Wall shear capacity was determined for all applicable loading conditions in accordance with Chapter 22 of ACI 318. The calculations, not contained in this article, showed that plain concrete was adequate to support shear forces as determined by either SOM or FEM analyses. In all cases, ACI Eq. (22-8), $V_u \le \phi V_c$, was easily satisfied using ACI Eq. (22-9), with ϕ = 0.65 as required for structural plain concrete. Note that shear friction analysis should apply at cold joints at the base of walls when there is no key or continuity between wall and footing concrete placements.

Wind overturning and uplift analysis

Again omitting the details for brevity, M_o, the overturning moment, was found to be 53.3 k-ft (72 kN-m). Conservatively assuming that resisting moment is provided by the mass of the side walls only, the capacity of the resisting moment M_r is 121 k-ft (160 kN-m).

$$M_r/M_o = 121/53.3 = 2.3 > 1.5 \text{ required } \therefore \text{ OK.}$$

Wall analysis of the components and cladding

According to ASCE 7-98, a windward wall section with no openings was isolated for the analysis of loading on the components and cladding. Resulting M_x and M_y moments were found for the two loading conditions: LC#3 = $1.05D + 1.275W$ and LC#4 = $0.9D + 1.3W$, where W is the applied wind load and D is the applied dead load. A components and cladding velocity pressure of 68 lb/ft² (3.3 kPa) was applied to a 2-D FEM model of the solid 50 ft (15 m) wall that was fixed at the base and simply supported along the remainder of the perimeter. The maximum M_x for either loading condition was found to be 0.46 k-ft/ft (2.1 kN-m/m) in the positive moment regions (in the upper half of the wall) and 0.49 k-ft/ft (2.2 kN-m/m) in the negative moment regions (at the base of the wall). In comparison, by conservatively applying $w\ell^2/8$ for a simply supported uniform load model, moment values for LC#3 and LC#4 were 0.88 and 0.90 k-ft/ft (3.9 kN-m/m and 4.0 kN-m/m), respectively. Axial dead loads were estimated at 30 lb/ft² (1.4 kPa) and included wood trusses, plywood sheathing, roofing, drywall ceiling, and concrete roof tile. The total dead load per foot of wall (including 1 ft [300 mm] of roof overhang) is then

w_d = (0.03 k/ft^2)(13 ft) = 0.39 k/ft (5.7 kN/m)

For self weight of 1/2 wall height

w_d = (0.15 k/ft^3)(4.5 ft)(0.34 ft) = 0.23 k/ft (3.4 kN/m)

and then

w_d = 0.62 k/ft (9.1 kN/m)

is the total axially applied dead load.

ICF-P analysis

Applying the load factors for LC#3 and LC#4 and the SOM analysis, the axial force and moment, respectively, applied to the wall are

LC#3: P_u = 1.05(0.62 k/ft) = 0.65 k/ft (9.5 kN/m)
M_u = 0.88 k-ft/ft (3.9 kN-m/m)

LC#4: P_u = 0.9(0.62 k/ft) = 0.55 k/ft (8.0 kN/m)
M_u = 0.90 k-ft/ft (4.0 kN-m/m)

The axial load capacity for ICF-P walls, where A_1 is the loaded area and ℓ_c is the vertical distance between supports

$$P_n = 0.60f_c'[1 - (\ell_c / 32h)^2]A_1 \quad \text{(ACI Eq. (22-5))}$$
$$= 24.9 \text{ k (111 kN)}$$

The moment capacity of the ICF-P walls

$$M_n = 0.85f_c'S = 6.8 \text{ k-ft (9.2 kN-m)} \quad \text{(ACI Eq. (22-3))}$$

where S = 32 in.^{3} (52,000 mm^3)

The interaction, using ϕ = 0.65, is

$$P_u / \phi P_n + M_u / \phi M_n \leq 1 \quad \text{(ACI Eq. (22-6))}$$

For LC#3: $P_u / \phi P_n + M_u / \phi M_n$ = 0.24 < 1.0 ∴ OK.
For LC#4: = 0.24 < 1.0 ∴ OK.

On the tension face

$$M_u / S - P_u / A_g \quad \text{(ACI Eq. (22-7))}$$
$$\leq 5\phi\sqrt{f_c'} = 178 \text{ psi (8.5 kPa)}$$

where A_g = 48 in.^{2} (3100 mm^2)

For LC#3: $M_u / S - P_u / A_g$ = 0.32 ksi (2.2 MPa) > 0.178 ksi (1.2 MPa) ∴ NG.
For LC#4: = 0.33 ksi > 0.178 ksi ∴ NG.

Thus, the 4-in.-thick (100 mm) plain structural concrete ICF-P design would not work for this example. When using the moment values obtained from the FEM analysis, however, M_u = 0.49 k-ft/ft (2.2 kN-m/m) for both loading conditions and ACI Eq. (22-6) and (22-7) are satisfied.

ICF-R analysis

For ICF-R walls for either LC#3 or LC#4, β_d = 1.0, I_g = 64 in.^{4} (26,000,000 mm^4), and EI = 39,960 k-in.^{2} (645 kN-mm^2). According to ACI 10.12.1, k = 1.0, P_{cr} = 33.8 k (150 kN) (ACI Eq. (10-10)), and C_m = 1.0 (ACI 10.12.3.1).

LC#3, using the SOM analysis, gives P_u= 0.65 k/ft (9.5 kN/m) and the magnified moment (with δ = 1.03 > 1.0), M_{mu} = 0.91 k-ft/ft (4.1 kN-m/m). From FEM analysis, M_{mu} = 0.50 k-ft/ft (2.2 kN-m/m).

LC#4, using SOM, gives P_u= 0.55 k/ft (8.0 kN-m/m) and a magnified moment (δ = 1.02) M_{mu} = 0.92 k-ft/ft (4.1 kN-m/m). From FEM analysis M_{mu} = 0.50 k-ft/ft (2.2 kN-m/m).

Design procedures use these values of P_u and M_{mu} with axial load and bending force interaction diagrams. For FRC walls, force interaction diagrams can be constructed as follows.

CONSTRUCTION OF FORCE INTERACTION DIAGRAM FOR FRC

Axial loading for one- or two-story residential buildings rarely controls design. Therefore, only that portion of the force interaction diagram that lies below balanced failure conditions needs to be considered. For pure bending (no axial load), the fully plastic bending moment capacity per foot of FRC wall can be expressed as a function of ARS and wall thickness h. Applying the capacity reduction factor ϕ which for no axial loading can be taken as 0.9, $\phi M_p = 1.8h^2$ (ARS).

Because the ARS is relatively small compared with the compressive strength of the concrete, the axial load at balanced failure is relatively high. Using ACI Eq. (22-4) and (22-5), with ϕ = 0.65 and the concrete strength f_c' reduced by ARS, a value predictably lower than the balanced failure load can be determined as

$$P_u = \phi P_n = \quad \text{(ACI Eq. (22-5))}$$
$$\phi 0.60f_c'[1 - (\ell_c / 32h)^2]A_1$$

where A_1, the loaded cross-sectional area per foot of wall, is $12h$ and ℓ_c, the unsupported length (in this example) is 108 in. (2.7 m), and the wall thickness is 4 in. (100 mm). Thus, the estimated balanced axial force is

$$P_{bu} = \phi P_{bn} = 0.00457(f_c' - \text{ARS})[1024(h) - (\ell_c^2 / h)]$$
$$= 15.1 \text{ k per ft of wall (220 kN/m)}$$

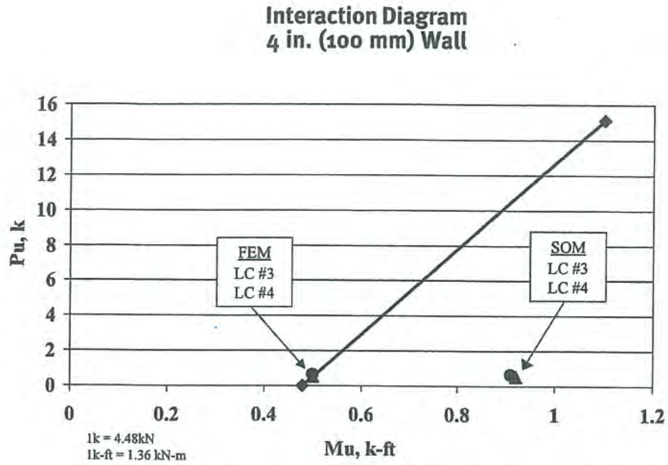

Fig. 8: Force interaction diagram for 4-in.-thick (100 mm) fiber-reinforced concrete insulating-form wall

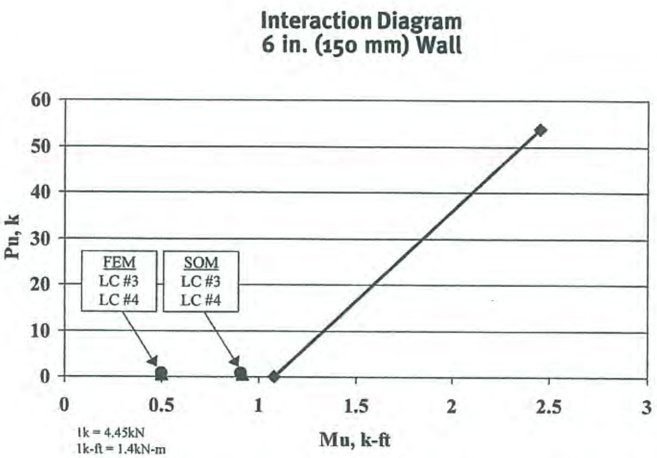

Fig. 9: Force interaction diagram for 6-in.-thick (150 mm) fiber-reinforced concrete insulating-form wall

The average compression stress is then $f_c = 15.1/A_1$, which for the 4 in. (100 mm) wall is 0.31 ksi (2.1 MPa). Under this compressive stress, tensile ARS is reached at the bending moment $\phi M_b = \phi S(\text{ARS} + 0.31)$ with the section modulus S for an uncracked section $I/c = 2h^2$ and ϕ conservatively 0.8. Considering the low axial loads that are applied, ϕM_b = 1.1 k-ft/ft (4.9 kN-m/m). The values P_{bu} = 15.1 k (220 kN) and M_{bu} = 1.1 k-ft (4.9 kN-m/m) establish a second point, one that is predictably below the balanced point, on the interaction diagram. In this example, the two points found for the construction of the interaction diagram, one along the horizontal (pure bending) axis and the other at or below the balanced point, are plotted as (0.00,0.48) and (15.1,1.1) and are shown in Fig 8. Repeating these steps for a 6 in. (150 mm) wall (for the same material properties) provides the interaction diagram shown in Fig 9.

FRC SATISFIES ACI 318 REQUIREMENTS

This example is not a final design and is intended only to demonstrate how FRC materials can be engineered to satisfy the requirements of ACI 318. Both SOM and FEM analytical procedures, and alternate assumptions regarding the manner in which internal forces are determined, were employed as part of the demonstration. No representations are made as to the completeness of this design because, for example, negative internal pressure wind loading conditions were not considered.

FRC has properties that are suited to the application of plastic analysis and design theory. Localized yielding, force redistribution, and elastic reloading are among the most important of these properties. Based on the example analysis, the following conclusions apply:

1. The interaction between axial and bending forces for that portion of the interaction which represents failure in the flexural mode for a 4 in. (100 mm) ICF-FRC wall having f_c' = 3 ksi (20 MPa) and ARS = 0.2 ksi (1.4 MPa) is shown as a straight line in Fig 8. The wind loading conditions LC#3 and LC#4 are shown as two points which, for this example, lie close to one another near the bottom of the diagram. These loading conditions each fall beyond the interaction capacity (below and to the right) when applying an SOM analysis. Wind moments by the FEM analysis, which models the wall top support condition as pinned and the bottom support conditions as fixed, reduces the design moments by approximately one half. In this case, the combined force interaction still falls on and outside the capacity limit of the 4 in. (100 mm) wall. The interaction diagram shifts position by varying the design parameters h and ARS with the latter being a function of the FRC system chosen.
2. When redesigned as a 6 in. (150 mm) ICF-FRC wall, but still using ARS = 0.2 ksi (1.4 MPa), the system satisfies the design criteria as shown by the interaction diagram and forces plotted in Fig 9.
3. If an initial elastic analysis predicts forces that exceed the capacity of either the chosen wall or support systems, then analysis using yield lines formed as moment-resistant hinges placed at critical locations for the affected sections can be employed. In any case, if no collapse mechanism is predicted, then the static theorem of plastic analysis and design assures that the force distribution for that particular analysis is both safe (no collapse) and statically admissible (in equilibrium). Thereafter, appropriate serviceability conditions can be addressed.